



## Magmatic differentiation processes at Merapi Volcano: inclusion petrology and oxygen isotopes

Valentin R. Troll<sup>a,\*</sup>, Frances M. Deegan<sup>a,b</sup>, Ester M. Jolis<sup>a</sup>, Chris Harris<sup>c</sup>, Jane P. Chadwick<sup>d</sup>, Ralf Gertisser<sup>e</sup>, Lothar M. Schwarzkopf<sup>f</sup>, Anastassia Y. Borisova<sup>g</sup>, Ilya N. Bindeman<sup>h</sup>, Sri Sumarti<sup>i</sup>, Katie Preece<sup>j</sup>

<sup>a</sup> Dept. of Earth Science, CEMPEG, Uppsala University, Villavägen 16, SE-752 36 Uppsala, Sweden

<sup>b</sup> Laboratory for Isotope Geology, Swedish Museum of Natural History, 104 05 Stockholm, Sweden

<sup>c</sup> Dept. of Geological Science, University of Cape Town, Rondebosch 7701, South Africa

<sup>d</sup> Dept of Petrology (FALW), De Boelelaan 1085, Amsterdam, The Netherlands

<sup>e</sup> School of Physical and Geographical Sciences, Keele University, Keele, ST5 5BG, UK

<sup>f</sup> GeoDocCon, Unterpferdt 8, 95176 Konradsreuth, Germany

<sup>g</sup> Observatoire Midi-Pyrénées, Université Toulouse, 14 Avenue E. Belin, 31400 Toulouse, France

<sup>h</sup> Dept. of Geological Sciences, 1272 University of Oregon, Eugene, OR 97403, United States

<sup>i</sup> Volcano Investigation and Technology Development Institution, Yogyakarta, Indonesia

<sup>j</sup> School of Environmental Sciences, University of East Anglia, Norwich, NR4 7TJ, UK

### ARTICLE INFO

#### Article history:

Received 5 March 2012

Accepted 2 November 2012

Available online 9 November 2012

#### Keywords:

Merapi Volcano

Magmatic and crustal inclusions

Oxygen isotopes

Crustal contamination

### ABSTRACT

Indonesian volcano Merapi is one of the most hazardous volcanoes on the planet and is characterised by periods of active dome growth and intermittent explosive events. Merapi currently degasses continuously through high temperature fumaroles and erupts basaltic-andesite dome lavas and associated block-and-ash-flows that carry a large range of magmatic, coarsely crystalline plutonic, and meta-sedimentary inclusions. These inclusions are useful in order to evaluate magmatic processes that act within Merapi's plumbing system, and to help an assessment of which phenomena could trigger explosive eruptions. With the aid of petrological, textural, and oxygen isotope analysis we record a range of processes during crustal magma storage and transport, including mafic recharge, magma mixing, crystal fractionation, and country rock assimilation. Notably, abundant calc-silicate inclusions (true xenoliths) and elevated  $\delta^{18}\text{O}$  values in feldspar phenocrysts from 1994, 1998, 2006, and 2010 Merapi lavas suggest addition of limestone and calc-silicate materials to the Merapi magmas. Together with high  $\delta^{13}\text{C}$  values in fumarole gas, crustal additions to mantle and slab-derived magma and volatile sources are likely a steady state process at Merapi. This late crustal input could well represent an eruption trigger due to sudden over-pressurisation of the shallowest parts of the magma storage system independently of magmatic recharge and crystal fractionation. Limited seismic precursors may be associated with this type of eruption trigger, offering a potential explanation for the sometimes erratic behaviour of Merapi during volcanic crises.

© 2012 Elsevier B.V. All rights reserved.

### 1. Introduction

Arc magmas typically display geochemical variations indicating involvement of crustal material during their petrogenesis (e.g., Hildreth and Moorbath, 1988; Davidson et al., 1990; Gertisser and Keller, 2003a). However, identification of a crustal component in magma genesis through, e.g., the use of whole rock Sr, Nd and Pb isotopes, provides limited information about where and when this contamination was introduced. Concerning the timing of contamination, two models are widely considered (cf. Wilson, 1997): i) crustal material may be derived from the subducted slab and added to the source of the arc magma (*source contamination*); and ii) crustal material may be added via upper crustal assimilation, as magma ascends above the subducted

plate (*crustal contamination*). On the basis of Sr–Nd–Pb isotopes in continental arcs (ocean–continent subduction), both contamination models appear significant (e.g., Hildreth and Moorbath, 1988; Davidson et al., 1990; Ellam and Harmon, 1990). For island arcs (ocean–ocean subduction), however, source contamination is generally assumed to be far more important (e.g., Arculus and Powell, 1986; Plank and Langmuir, 1998; Gertisser and Keller, 2003a; Debaille et al., 2006), although some researchers have proposed models involving crustal contamination for island arcs (Arculus and Johnson, 1981; Davidson, 1995; Thirlwall et al., 1996; Chadwick et al., 2007). Here we present a petrological synopsis of juvenile lavas, crystals, plutonic and crustal fragments and inclusions from the Merapi 1994, 1998, 2006, and 2010 block-and-ash-flow and ash deposits and report on their petrographic characteristics and their oxygen isotope compositions. Our data provide information on the rock types present in the Merapi subvolcanic environment and the processes that operate in its plumbing system. Based on our petrological and stable

\* Corresponding author.

E-mail address: [valentin.troll@geo.uu.se](mailto:valentin.troll@geo.uu.se) (V.R. Troll).

isotope study, we argue that shallow-level crustal processes, particularly late-stage limestone contamination, can play a considerable role in helping to explain both, the oxygen isotope variability in Merapi erupted products and Merapi's propensity for sudden explosive behaviour.

## 2. Geological setting

Merapi Volcano is situated in Central Java within the active volcanic front of the Sunda arc, which results from the northward subduction of the Indo-Australian plate beneath the Eurasian plate at a rate of about 6.5 to 7 cm/yr near Java (Fig. 1) (Hamilton, 1979; Jarrard, 1986). Like the majority of the large Quaternary stratovolcanoes of Central and East Java, Merapi rises from the lowlands of the Solo Zone (van Bemmelen, 1949), a longitudinal depression in East-Central Java that consists of Tertiary and older rocks underneath a lithologically variable cover of alluvial deposits. The subvolcanic basement of Merapi consists of immature arc crust approximately 20 km thick (Curray et al., 1977; Jarrard, 1986). The upper part of this crust comprises a thick sequence of Cretaceous to Tertiary limestones and marls that crop out in the immediate surroundings of Merapi (Fig. 1H; van Bemmelen, 1949; Smyth et al., 2005). The thermally metamorphosed equivalents of these crustal lithologies can be found as abundant calc-silicate inclusions (xenoliths) in Merapi lavas (Clocchiatti et al., 1982; Camus et al., 2000; Gertisser and Keller, 2003a; Chadwick et al., 2007; Deegan et al., 2010; Troll et al., 2012).

Merapi's eruptive activity is currently characterised by dome growth, small-volume pyroclastic flows (BAFs) and associated ash fall that is compositionally restricted to mainly basaltic-andesite compositions ranging in SiO<sub>2</sub> from 51.5 to 56.5 wt.% (Fig. 1) (Gertisser and Keller, 2003b). Dome growth periods may last for several years but are frequently interrupted by shorter explosive events (VEI = 1 to 4; see Voight et al., 2000) lasting for only hours to days (e.g., Andrestuti et al., 2000; Camus et al., 2000; Newhall et al., 2000; Voight et al., 2000; Surono et al., 2012). Merapi's long-term record suggests that frequent plinian, sub-plinian and vulcanian eruptions (0.11–0.26 km<sup>3</sup> volume and VEI = 4) have occurred in the past and are thus likely to occur again in the future (Andrestuti et al., 2000; Camus et al., 2000; Newhall et al., 2000; Gertisser and Keller, 2003b; Gertisser et al., 2012). It is estimated that Merapi has caused ≥ 1300 fatalities in the last 100 years alone, a period of time considered to be of fairly low explosivity compared with Merapi's long term record (Newhall et al., 2000; Gertisser et al., 2012). In fact, cycles last several hundred years with at least three major cycles occurring in the past 2000 years (Gertisser and Keller, 2003b; Gertisser et al., 2012). Based on the volcano's previous record, recent eruptive style, and magma chemistry, Gertisser and Keller (2003b) argued that Merapi is currently at the beginning of a major phase of increased eruptive activity. Indeed, an increase in Merapi's activity will pose formidable problems to risk assessment and disaster mitigation in the decades to come (e.g., Andrestuti et al., 2000; Itoh et al., 2000; Thouret et al., 2000; Charbonnier and Gertisser, 2008). This is in part because of Merapi's erratic behaviour, but also due to the fact that Java is the island with amongst the highest population density in the world (1000 people/km<sup>2</sup>) and the area around Merapi Volcano is particularly densely populated (Yogyakarta ≥ 3.5 M inhabitants). In terms of human mortality, Merapi is one of the top ten deadly volcanoes worldwide (Witham, 2005), which is also reflected in the “disaster subculture” that has evolved there (Donovan and Suharyanto, 2011). Merapi is also notable by elevated <sup>87</sup>Sr/<sup>86</sup>Sr values measured in its lavas relative to other Sunda arc volcanoes (Turner and Foden, 2001) and we hence hypothesise that Merapi's exceptionally dangerous behaviour compared to other Javanese volcanoes may be linked to assimilation of upper crustal carbonates.

Although dome growth events are relatively long-lived and can be monitored, prediction of short-lived explosive events is often more difficult as these may build up in only hours to days and precursor seismic signals at Merapi cannot always be directly translated into sub-surface

processes (e.g., Ratdomopurbo and Poupinet, 2000; Richter et al., 2004; Budi-Santoso et al., 2013; Jousset et al., 2013; Surono et al., 2012). It is believed that dome growth is generally associated with deep and shallow earthquakes (i.e., volcanotectonic seismic events: VTs), but some pyroclastic eruptions seem to be associated with mainly shallow hybrid seismic events and tremors (Hidayat et al., 2000; Ratdomopurbo and Poupinet, 2000). Those eruptions associated with deep VT earthquakes, suggest magma migration at depth within the volcanic edifice, probably supplying shallow level magma reservoirs with fresh magma from below. Eruptions associated with shallow or near-surface seismic activity (hybrid earthquakes, multi-phase events, and tremors), in turn, point towards a set of shallow processes that can also act as an eruption trigger in high-level, upper crust-hosted magma chamber(s) and conduits. For example, shallow tremors are often considered to reflect near surface magma expansion due to vesiculation (cf. Ratdomopurbo and Poupinet, 2000). An aseismic zone was identified at a depth of about 2.5 to 3 km (e.g., Ratdomopurbo and Poupinet, 2000), supporting the existence of at least a transient shallow magma pocket beneath Merapi, consistent with recent petrological and mineral barometry studies that suggest a relatively high-level, quasi-steady state magma system beneath the volcano (Gertisser and Keller, 2003b; Chadwick, 2008; Preece et al., 2012). An independent, but complementary line of evidence to glean insight into the inner workings of Merapi's plumbing system is the record of eruptive products and the inclusions contained within them. At Merapi, inclusions comprise igneous varieties (volcanic and plutonic) and variably metamorphosed fragments of sedimentary country-rock (mainly calc-silicates, meta- and volcanoclastic sediments) (Figs. 2 and 3). In particular, the variety of calc-silicate xenoliths present in Merapi eruptives allows us to link shallow magma chamber processes with experimental timescales of magma–carbonate interaction (Deegan et al., 2010, 2011) and gas chemistry of Merapi's fumaroles (Allard, 1983; Troll et al., 2012), thus forging a link between subsurface chamber processes, gas emission, and eruptive behaviour of the volcano.

## 3. Analytical techniques

Lava and inclusion samples were collected from block-and-ash-flow deposits and ash fall layers, comprising the 1994, 1998, 2006, and 2010 eruptive cycles. Inclusions are exclusively from block-and-ash-flows and usually range from a few centimetres across to, in rare cases, several decimetres across.

Samples were washed and cut in the laboratory removing weathered or altered materials carefully. Samples were then crushed in a jaw crusher and minerals or rock fragments were hand-picked from the crushed materials under a stereo-binocular microscope, making sure that only pristine materials were used for analysis. Powders for conventional oxygen isotope analysis were produced from the sand-sized crush using an agate ball mill. All oxygen isotope compositions are given in standard  $\delta$ -notation,  $\delta = (R_{\text{sample}}/R_{\text{standard}} - 1) \times 1000$ , where  $R = {}^{18}\text{O}/{}^{16}\text{O}$ , relative to SMOW.

The majority of oxygen-isotope ratios of whole rock samples ( $n = 24$  including lavas, inclusions, and crustal samples) and mineral separates ( $n = 12$ ) were determined using a Thermo DeltaXP mass spectrometer at the University of Cape Town (UCT) after extraction of oxygen by conventional methods using ClF<sub>3</sub> as the reagent (Borthwick and Harmon, 1982). Further details of the extraction methods for oxygen from silicates employed at UCT have been described by Vennemann and Smith (1990), and Fagereng et al. (2008). Samples were run in batches of eight, along with duplicate samples of the internal quartz standard NBS-28. The analytical error for  $\delta^{18}\text{O}$  is estimated to be  $\pm 0.1\%$  ( $1\sigma$ ) based on long term-duplication of NBS-28.

Pyroxene and feldspar separates from samples M07-53, M11-01, and the MC cumulate ( $n = 8$ ) were analysed by laser fluorination at UCT (see Harris and Vogeli, 2010 for the method). Each sample was reacted in the presence of ~10 kPa BrF<sub>5</sub> and the purified O<sub>2</sub> was collected onto a 5 Å

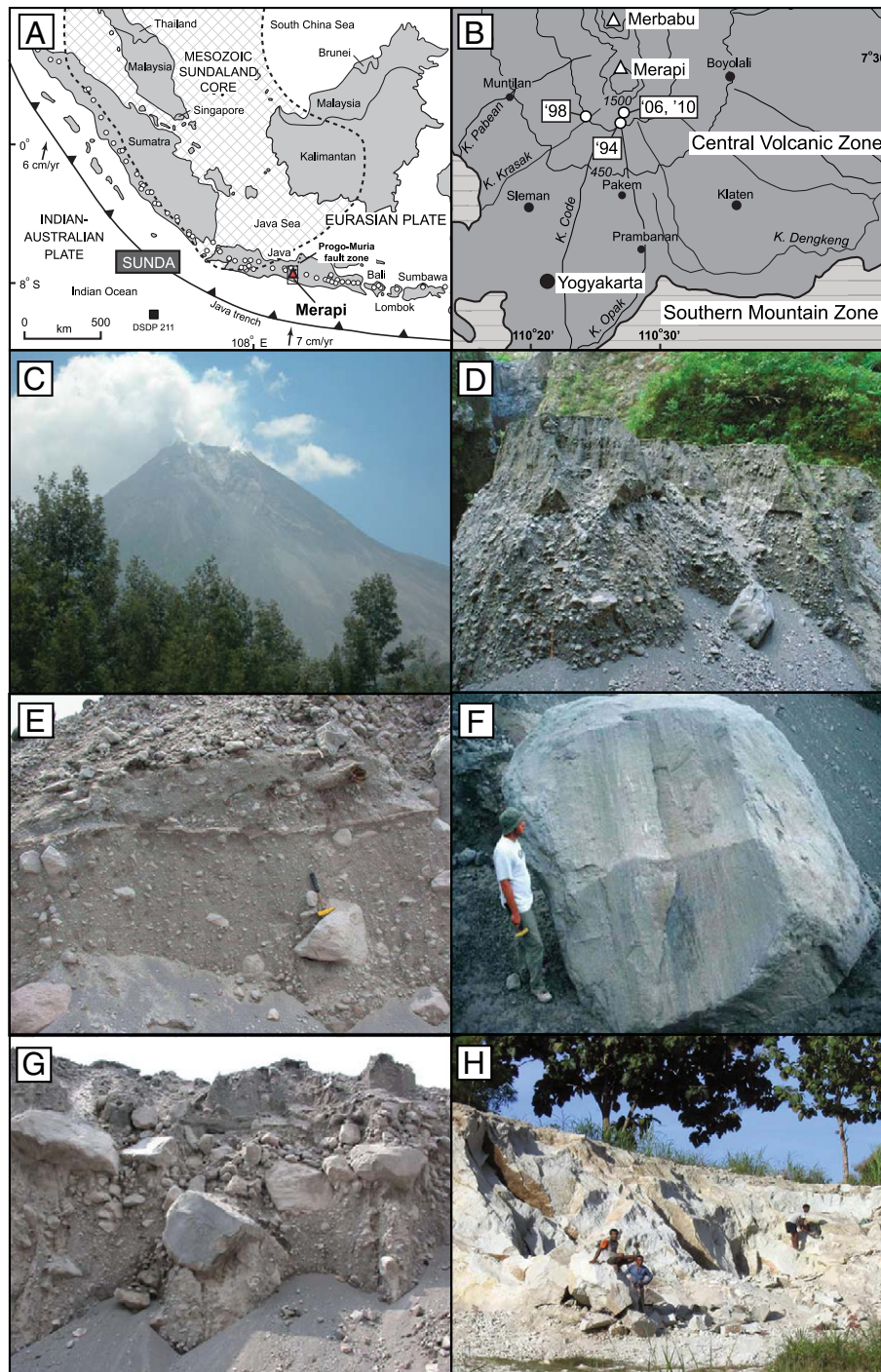


**Fig. 1.** (A) Overview map of the Sunda arc, Indonesia. Open circles represent active volcanic centres. Merapi Volcano in Central Java is highlighted. Cross-hatched area represents Mesozoic continental crust (the Sundaland terrane), which probably extends as far as Central Java, although under an increasingly thicker sedimentary cover (modified after Gertisser and Keller, 2003a using crustal boundaries from Smyth et al., 2005 and references therein). (B) Simplified locality map of Merapi and surroundings. Nearby major population centre is the city of Yogyakarta, c. 25–30 km to the south (zoom in from box in A). Sample locations for this study are indicated: 1994 and 1998 xenolith-bearing block-and-ash flows (BAF) on the south flanks of Merapi, labelled “94” and “98”, respectively, and the 2006 and 2010 sampling locations (at the village of Kaliatem, labelled “06” and “10”, respectively). (C) View of Merapi Volcano from a distance; (D) Field appearance of the block-and-ash-flow from 1994 eruption; (E), (F) and (G) Field appearance of the block-and-ash-flow deposits from the 1998 eruption (compare Schwarzkopf et al., 2005); (H) Limestone quarry in the western outskirts of Yogyakarta.

molecular sieve contained in a glass storage bottle. The O-isotope ratios of samples analysed using laser fluorination were measured on O<sub>2</sub> gas. Measured values of the internal standard MON GT (Harris et al., 2000) were used to normalise the raw data and correct for drift in the reference gas.

The average difference in  $\delta^{18}\text{O}$  values of duplicates of MON GT analysed was 0.13‰ (n = 26), and corresponds to a 2 $\sigma$  value of 0.16‰.

Limestone samples M-LST-1 to 3 were reacted with 100% phosphoric acid at 25 °C. The CO<sub>2</sub> extracted was analysed for both carbon and oxygen

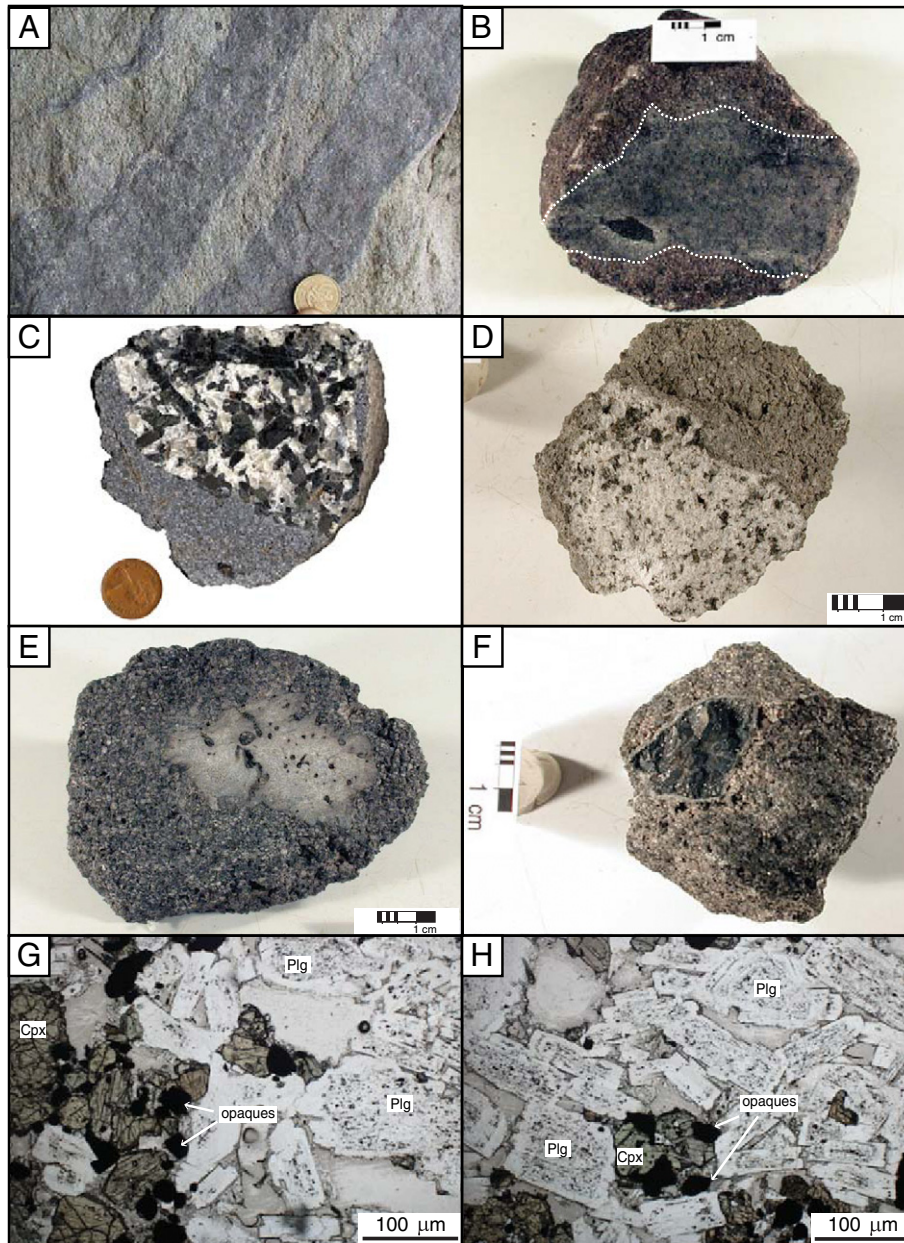


**Fig. 2.** Representative Merapi igneous inclusion types: (A) Schlieren and streaks of 'andesite in andesite'. The lenticular shapes of the andesite schlieren indicate a fluid–fluid relationship between the two andesite types; (B) 'Basalt in andesite' with chilled fluid contact with host rock (dashed lines); (C) Coarse grained gabbroic cumulate; (D) Diorite; (E) Partly resorbed microgabbro. C, D and E provide evidence for crystal accumulation in the plutonic environment beneath Merapi; (F) 'Amphibole megacrysts'. The amphibole megacrysts usually display reaction rims with host basaltic andesite; (G) and (H) Photomicrographs (PPL) of felsic plutonic inclusions (Cpx: clinopyroxene; Plg: plagioclase).

and data were corrected using a fractionation factor of 1.01025. Data were normalised to the V-SMOW and V-PDB scales and calibrated against NBS-19. Further details on the analytical procedure are described in Potts et al. (2009).

Oxygen isotopic measurements of bulk ash samples from the 2010 eruption ( $n=4$ ; M2010-1 to 4) and plagioclases ( $n=2$ ; M2010K and M2010-GR) were performed using the laser fluorination technique at the University of Oregon (see Bindeman et al., 2008). Samples were heated with an infrared (9.6  $\mu\text{m}$ ,  $\text{CO}_2$ ) laser in the presence of purified  $\text{BrF}_5$  to release oxygen. The oxygen was then converted to  $\text{CO}_2$  gas by using hot graphite and then analysed with the IRMS in dual inlet mode (see Borisova et al., 2012, for procedural details). Four to seven garnet standards ( $\delta^{18}\text{O}=6.52\text{‰}$ , UOG garnet) were analysed together with the unknowns during each of seven analytical sessions. The standards precision is better than  $\pm 0.1\text{‰}$  ( $1\sigma$ ).

## 4. Petrology of lavas and inclusions

### 4.1. Basaltic-andesite host lavas

Recent erupted products at Merapi Volcano (1994–2010) are fairly typical of an intermediate arc volcano, being basaltic-andesite in composition and highly plagioclase-porphyrific. Merapi basaltic-andesite is medium to dark grey in colour and contains up to 60% phenocrysts by volume. The phenocryst assemblage is dominated by plagioclase, which is typically complexly zoned, with  $\leq 5\%$  pyroxene (clinopyroxene plus minor orthopyroxene), Fe-oxides, and amphibole. Many individual plagioclase crystals exhibit large within-crystal compositional variations in terms of both anorthite content ( $\text{An}_{34-95}$ ) and the Sr isotope ratio of individual zones ( $^{87}\text{Sr}/^{86}\text{Sr}$  ranges from  $0.70568 \pm 6$  to  $0.70627 \pm 12$ ) (Chadwick et al., 2007). The groundmass surrounding the crystals is

microcrystalline to glassy. The inclusions hosted by Merapi basaltic-andesite lavas can be categorised into two broad groups: igneous and meta-sedimentary (Fig. 2). In the next section, we describe each group separately.

#### 4.2. Igneous inclusions

The range of igneous inclusions is rather wide and comprises the following types:

- (i) Schlieren and streaks in basaltic-andesite lavas occur frequently, showing lobate margins and ‘fluid–fluid’ relationships, which we have termed ‘andesite in andesite’ texture or ‘highly crystalline basaltic-andesite’ (Fig. 2A). They do not show chilled margins and document slightly different facies of andesitic magmas that mixed and mingled only shortly prior to final solidification.
- (ii) Rare basaltic enclaves occur that show lobate to strung-out contacts against the host basaltic-andesites. These frequently show a chilled margin, recording a considerable temperature difference between the two liquids, implying partial freezing of the enclave in the host lava (Fig. 2B).
- (iii) Plutonic inclusions and fragments comprise coarse- to medium-grained gabbro to diorite compositions (Fig. 2C–E and G–H), with a range of textures from massive to fine-scale mineral layering present. Resorption features are present in several samples, documenting that some of the plutonic inclusions are not in equilibrium with the host lavas.
- (iv) Amphibole megacrysts, up to 8 cm in size, with internal zoning and pronounced reaction rims occur in the basaltic-andesite host, again reflecting dis-equilibrium between these and the lava in which they are found (Fig. 2F).
- (v) Lastly, angular to resorbed basaltic to intermediate inclusions (e.g., dolerites) with various degrees of thermal and hydrothermal alteration features, thermo-metamorphic recrystallisation, and resorption textures are occasionally found, likely reflecting older igneous products such as dykes or other minor intrusions.

#### 4.3. Calc-silicate inclusions (xenoliths)

Abundant calc-silicate xenoliths (thermally metamorphosed limestones, partially infiltrated by basaltic-andesite and with well-developed reaction rims), are frequent in the Merapi basaltic-andesite deposits (Fig. 3A–D). These calc-silicate inclusions are true crustal xenoliths and are composed of a characteristic diopside + wollastonite mineralogy with traces of quartz, tremolite and garnet in several of the samples (Chadwick, 2008). Mineral determination by X-ray diffraction (XRD; see Chadwick et al., 2007 for analytical details) indicate an increase in wollastonite content towards the cores of these inclusions (up to 74%) and a dominance of diopside and anorthite in the rims (diopside up to 60% in rims) (Fig. 3E). This is indicative of an advanced stage of magma–xenolith interaction, i.e., it reflects the conversion of the original limestone mineralogy to a gradually more “lava-like mineralogical composition” (cf. Bowen, 1928; Fulignati et al., 2004; Gaeta et al., 2009; Mollo et al., 2010). Calc-silicate inclusions have also been found as small xenoliths in type (iii) diorite inclusions, confirming their availability in the plutonic environment. At direct magma–calc-silicate interfaces, the basaltic-andesite host rock is often extremely vesicular, probably indicating liberation of volatiles due to magma–carbonate interaction (cf. Deegan et al., 2010; Fig. 3). Besides the abundant calc-silicate inclusions, rare thermally

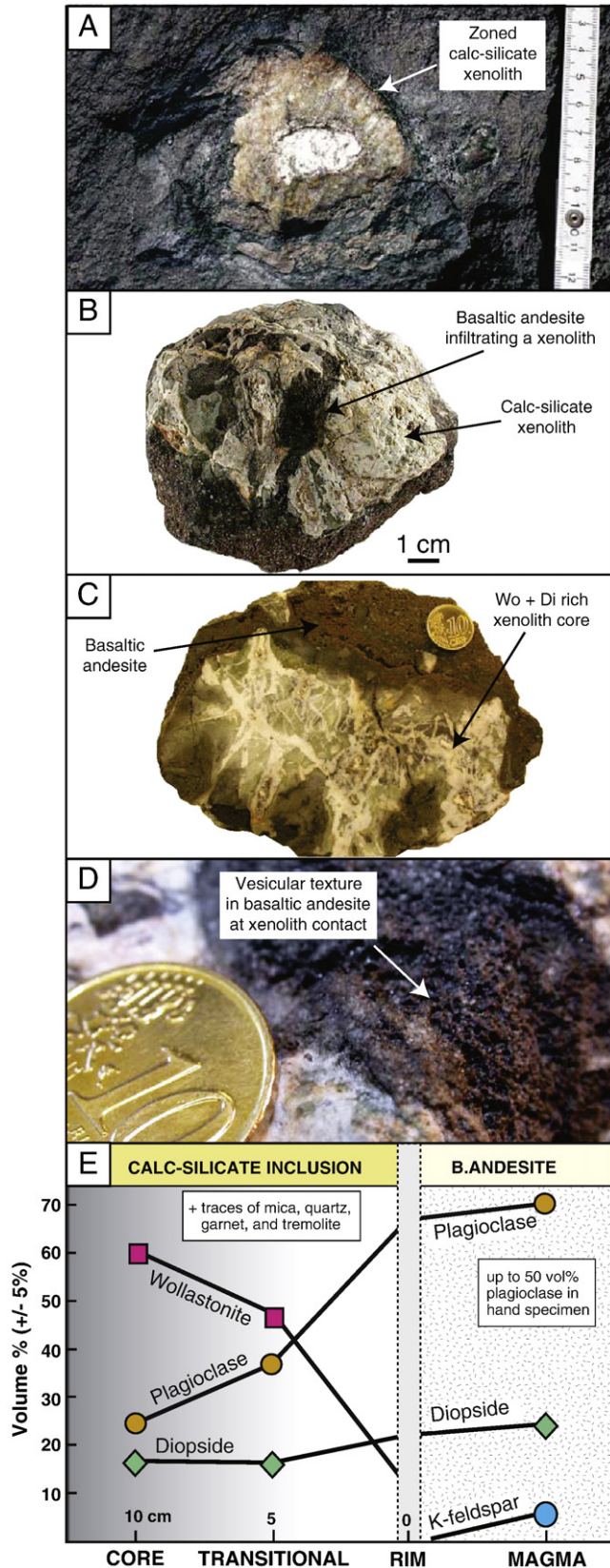


**Fig. 3.** (A) Field photograph of a Merapi calc-silicate inclusion in a BAF deposit showing mineralogical zoning indicative of intense interaction between calc-silicate and host magma. Wollastonite is found in the core grading into a diopside-rich assemblage that eventually blends with the surrounding basaltic-andesite. (B) and (C) Hand specimen photographs of a representative Merapi calc-silicate inclusion showing textural evidence for interaction between the inclusion and surrounding basaltic-andesite magma. (D) Close up of the inclusion shown in (B) and (C); Note the bubbly texture at the contact zone with the magma pointing to gas release from the carbonate-rich inclusion into the intruding melt. (E) Mineralogical core to rim profile through a typical calc-silicate inclusion based on XRD analysis (see Troll et al., 2012). Note a decrease from the centre to rim in wollastonite, but an increase in plagioclase and diopside, indicating progressive conversion of the crustal inclusion to a more ‘lava-like’ composition (see text for details).

overprinted siliciclastic and volcanoclastic inclusions occur that testify to the presence of some inhomogeneity within or above the sub-Merapi carbonate bedrock sequence.

#### 4.4. Volcanoclastic inclusions

Volcanoclastic inclusions are less common than the calc-silicates inclusions. They are fine (<1 mm) to medium (1–5 mm) in grain size and are metamorphosed silicic sediments composed primarily of feldspar and quartz. A more detailed petrographic description of these inclusions is given in Chadwick et al. (2007).

### 5. Results and calculations

#### 5.1. Oxygen isotope data

Oxygen isotope ratios of Merapi basaltic-andesite whole rocks, phenocrysts, plutonic and metasedimentary inclusions, and local limestone are listed in Table 1 (a and b). Whole-rock basaltic-andesite  $\delta^{18}\text{O}$  values range from  $+5.6 \pm 0.1\%$  to  $+8.3 \pm 0.1\%$  ( $n=11$ ), similar to values previously reported for Merapi (i.e.,  $+6.0$  to  $+8.3\%$ ; Gertisser and Keller, 2003a and Table 1a). Feldspar and pyroxene  $\delta^{18}\text{O}$  values range from  $+5.9 \pm 0.1\%$  to  $+7.9 \pm 0.1\%$  ( $n=11$ ) and from  $5.1 \pm 0.1\%$  to  $7.2 \pm 0.1\%$  ( $n=11$ ), respectively. These values are higher than typical mantle values ( $\delta^{18}\text{O}$  of average Indian Ocean type MORB =  $5.75 \pm 0.2\%$ ; Ito et al., 1987) and mafic arc melts ( $\delta^{18}\text{O} = 5.2$  to  $6.2\%$  cf. Eiler et al., 2000). Limestones from the local platform carbonate sequence ( $n=5$ , including two literature values) have  $\delta^{18}\text{O}$  between  $+18.9$  and  $+24.5$  ( $\pm 0.1\%$ ), characteristic of this type of rock (e.g., Hoefs, 1996). Calc-silicate inclusions in the lavas ( $n=10$ , including one literature value) show a comparatively narrow range of  $\delta^{18}\text{O}$  from  $+10.4$  to  $+14.7$  ( $\pm 0.1\%$ ) (Fig. 4).

#### 5.2. Assessing mineral–mineral and mineral–melt equilibria

A  $\delta$ – $\delta$  diagram is a useful way to investigate O-isotope equilibrium between co-existing minerals. Minerals in equilibrium within a rock suite are characterised by arrays that lie on a line of constant difference ( $\Delta$ , e.g.,  $\Delta_{\text{fsp-px}}$ ) in  $\delta^{18}\text{O}$  value between the two minerals (e.g., Gregory and Criss, 1986; Gregory et al., 1989), and hence constant temperature. Minerals in O-isotope disequilibrium will form steep arrays that cut these equilibrium lines (Fig. 5A). Several samples of the Merapi mineral pairs (M-BA06-KA4, M-BA06-KA5 and M11-01, Table 2), form an array with a negative correlation that indeed cuts across the equilibrium line.

The range in  $\Delta_{\text{fsp-px}}$  in the Merapi magmas spans between  $-0.2$  to  $+1.19$ , and this is plotted against  $\delta^{18}\text{O}$  value in Fig. 5B. This diagram shows that the plagioclase  $\delta^{18}\text{O}$  value increases with  $\Delta_{\text{fsp-px}}$ , whereas the  $\delta^{18}\text{O}$  value of pyroxene decreases, although this observation is not strictly systematic. In order to resolve the contribution of individual components, and bearing in mind that only a small number of  $\delta^{18}\text{O}$  mineral pairs is available, the difference in  $\delta^{18}\text{O}$  between feldspar and pyroxene phenocrysts can be interpreted in two different ways. The negative correlation observed in Fig. 5A can be explained as being caused by magmatic evolution from the same magma or very similar magmas. However, petrological features of Merapi lavas are consistent with mixing between magmas of similar compositions, (e.g., andesite in andesite) (Fig. 2). In this case, the difference in the  $\delta^{18}\text{O}$  values between feldspars and pyroxene phenocrysts would be semi-random and would reflect crystallisation from somewhat different magmas at different magma storage levels (see below). Regardless of the exact mechanism, the results at Merapi indicate that variable amounts of both fractional crystallisation and assimilation are required. The  $\delta^{18}\text{O}$  values in the feldspars, and many of the pyroxenes, are considerably higher than the values expected in a mantle-derived magma that evolved in a closed system (e.g., Sheppard and Harris, 1985; Hoefs, 1996; Bindeman,

**Table 1a**

Oxygen isotope composition of Merapi basaltic-andesite, and representative inclusions.

Sample type	Sample I.D.	$\delta^{18}\text{O}$ (w.r.)	$\delta^{18}\text{O}$ (px)	$\delta^{18}\text{O}$ (fsp)	
<i>Basaltic andesites</i>					
1998 BAFs	M-BA98-KA1	+7.7	+6.5		
	M-BA98-KA2	+7.1	+6.8	+7.8	
2006 BAFs	M-BA06-KA1	+6.9	+6.9	+7.4	
	M-BA06-KA2	+7.1	+6.6	+7.2	
	M-BA06-KA3	+7.5	+5.9		
	M-BA06-KA4	+6.1	+7.2	+7.0	
	M-BA06-KA5	+6.1	+6.7	+7.9	
	M07-53	+8.3	+5.4*	+5.9*	
2010 BAF	M11-01	+7.0	+5.1*	+6.3*	
2010 ash deposits	M2010K plg-1			+6.5#	
	M2010GR plg-2			+6.5#	
	M2010-1	+6.9#			
	M2010-2	+6.8#			
	M2010-3	+5.6#			
	M2010-4	+6.8#			
	Literature data† (Lava bulk rock)	M95-026	+6.4		
		M96-056	+6.6		
		M98-047	+6.9		
		M98-107	+6.9		
		M96-073	+6.3		
		M96-137	+6.8		+6.5
		M96-163	+8.3		+7.0
		M98-0532	+7.3		
M96-102		+6.9		+6.7	
M96-167		+6.0			
M97-021		+6.7			
M97-031		+7.0			
M97-0392		+6.2			
M97-053		+7.0		+6.8	
M98-030	+7.1		+6.6		
M98-031	+7.5		+6.6		
M98-066	+6.6				
M98-096	+6.5				
M96-142	+6.7				
M97-068	+6.3				
<i>Plutonic inclusions</i>					
(Bulk rock samples)	M-98-PX-101	+6.8			
	M-98-PX-102	+6.8			
	M-98-PX-108	+6.5			
Coarse grained cumulate	MC – cumulate		+5.4*	+6.0*	
	MC – replicate		+5.8*	+6.2*	
<i>Calc-silicate xenoliths</i>					
Bulk rock sample	8-c-3	+11.5			
Bulk rock sample	8-c-1c	+14.2			
Separated core wollastonite	M-XCS-1C	+14.1			
Separated rim diopside	M-XCS-1R	+11.0			
Separated core wollastonite	M-XCS-0C	+10.4			
Separated rim diopside	M-XCS-0R	+10.4			
Bulk rock sample	M-XCS-9	+11.9			
Literature data (bulk sample)†	MX-6	+11.5			
<i>Volcanoclastic xenolith</i>					
(Bulk rock samples)	M-XCS-2	+13.5			
	M-XCS-4	+14.7			

All values reported to one d.p. and in ‰ relative to SMOW. Abbreviations: "w.r.", whole rock; "px", pyroxene; "fsp", feldspar. Analytical error is given in the text and in Gertisser and Keller (2003a) and Troll et al. (2012), where applicable.

\* Analysed by laser fluorination at UCT.

# Analysed by laser fluorination at Univ. Oregon.

† Literature data taken from Gertisser and Keller (2003a) and Troll et al. (2012).

2008). This suggests that assimilation is a key processes, likely also responsible for the variations between mineral pairs (as discussed below).

To explain the observed decrease in the  $\delta^{18}\text{O}$  value in pyroxene, in turn, gradual magnetite fractionation in the system can be considered to occur, e.g., as microinclusions in the pyroxene crystals themselves (which would decrease the  $\delta^{18}\text{O}$  value of the analysed material). The

**Table 1b**  
Oxygen and carbon isotope composition of Merapi local crust.

Sample type	Sample I.D.	$\delta^{18}\text{O}$ (w.r.)	$\delta^{13}\text{C}$ (w.r.)
<i>Local crust</i>			
Volcanoclastic	J-VC-1	+12.5	
Limestone	M-LST-1	+24.0	-4.2
Limestone	M-LST-2	+24.5	-4.1
Limestone	M-LST-3	+24.1	-2.7
Literature data (Java limestone) <sup>†</sup>	MX99-1	+20.5	-2.2
Literature data (Java limestone) <sup>†</sup>	MX99-2	+18.9	-1.6

All values reported to one d.p. and in ‰ relative to SMOW. Abbreviations: “w.r.”, whole rock. Analytical error is given in the text and in Gertisser and Keller (2003a) and Troll et al. (2012), where applicable.

<sup>†</sup> Literature data taken from Gertisser and Keller (2003a) and Troll et al. (2012).

effect of  $\text{CO}_2$  liberated during crustal interaction would, moreover, increase the  $f\text{O}_2$  of the magma, which could have promoted increased magnetite fractionation, with progressively more microinclusions of magnetite becoming incorporated into the pyroxene crystals. These would lower the  $\delta^{18}\text{O}$  values of pyroxenes relative to the feldspars because magnetite has inherently lower  $\delta^{18}\text{O}$  values than silicate minerals, and is a potential cause of the observed negative correlation between plagioclase and pyroxene  $\delta^{18}\text{O}$  values. Magnetite microinclusions are difficult to recognise in these pyroxenes which appear dark and almost opaque under the binocular microscope, and hence magnetite microinclusions are unavoidable. Although a decrease in pyroxene  $\delta^{18}\text{O}$  values is possible due to an increase in the proportion of magnetite incorporation, the  $\delta^{18}\text{O}$  range displayed by Merapi pyroxenes spans over ca. 2‰ and would require the inclusion of excessive proportions of magnetite to explain the variation in full. Consider, for instance, that a mere 0.5‰ range in the data would require about 38% magnetite added, assuming that magnetite contains 66% of the O in pyroxene and that  $\Delta_{\text{px-mt}} = 2\text{‰}$  (Chiba et al., 1989). This is not consistent with the few magnetite crystals included in the pyroxenes observed in thin section and is hence unlikely to represent the main cause of the pyroxene  $\delta^{18}\text{O}$  variation. Another process that could explain the lowest pyroxene values may be the incorporation of some relatively low  $\delta^{18}\text{O}$  plutonic pyroxenes (as seen in Fig. 2). If so,

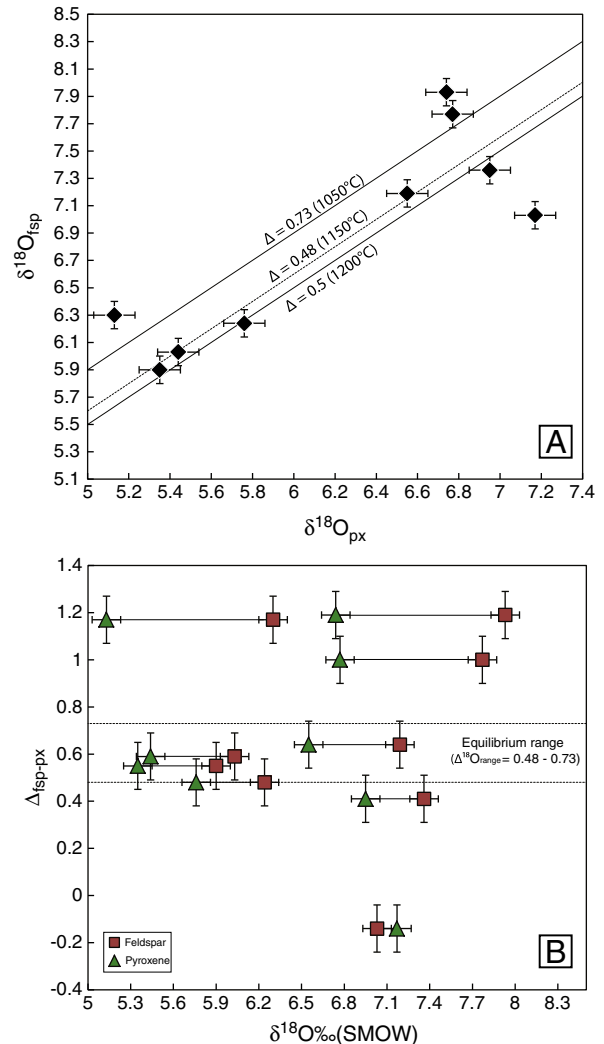


**Fig. 5.** (A) Plot of  $\delta^{18}\text{O}$  of feldspar vs.  $\delta^{18}\text{O}$  of pyroxene for Merapi samples where mineral pairs are available. Feldspar–pyroxene isotherms for 1200, 1150 and 1050 °C (corresponding to  $\Delta_{\text{fsp-px}}$  of 0.5, 0.48 and 0.73‰, respectively) are shown. The isotherms are calculated using the calibration of Chiba et al. (1989). (B) Plot of  $\Delta_{\text{fsp-px}}$  versus mineral  $\delta^{18}\text{O}$  value. Pairs of feldspar (squares) and pyroxene (triangles) from same rock sample are connected by a line.

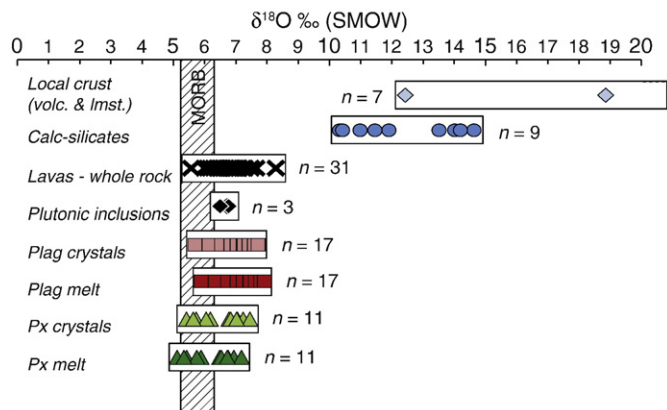


**Fig. 4.** Bar chart showing oxygen isotope variations in Merapi lavas (whole rock), mineral separates (pyroxene and feldspar) and their calculated melt compositions, igneous and metasedimentary inclusions, and local limestone and volcanoclastic crust. For comparison, the  $\delta^{18}\text{O}$  range of Indian Ocean type MORB ( $5.7 \pm 0.3\text{‰}$ ; Ito et al., 1987) is provided. Mean pyroxene and corresponding melt  $\delta^{18}\text{O}$  values are within the mantle range. Note, however, that the mean plagioclase and corresponding melt  $\delta^{18}\text{O}$  values are elevated from the mantle range, indicating increasing crustal influence concurrent with magma differentiation.

the samples would represent a mixture of andesite-derived and plutonic pyroxenes, the latter potentially overprinted at modest to high-temperatures.

Estimating the  $\delta^{18}\text{O}$  values of the melts in equilibrium with a mineral is another important step to evaluate the reasons for isotopic variations. The oxygen isotope compositions of the host magmas ( $\delta^{18}\text{O}_{\text{melt}}$ ) have been calculated from pyroxene and feldspar phenocryst  $\delta^{18}\text{O}$  values (Table 2) in order to assess the degree of variability in the magma  $\delta^{18}\text{O}$  value. We have assumed the following differences between mineral and magma:  $\Delta_{\text{px-melt}} = -0.3$  and  $\Delta_{\text{fsp-melt}} = 0.2$  (e.g., Kyser et al., 1981; Harris et al., 2005). The melt  $\delta^{18}\text{O}$  values range from 5.4 to 7.5‰ based on measured pyroxene data, and from 5.7 to 7.7‰ based on measured plagioclase data (Fig. 4). Although the ranges broadly overlap, the individual plagioclase–pyroxene pairs are as often in equilibrium as they are not (Table 2, Fig. 5). The difference in melt  $\delta^{18}\text{O}$  calculated from several pyroxene and feldspar therefore suggests that many pyroxene–feldspar pairs have not crystallised from the same magma and are likely to have formed in broadly different plutonic regimes. This is consistent with mineral barometry data presented in Chadwick (2008), where early and main pyroxene crystallisation occurs at a depth of 25 to

**Table 2**

Oxygen isotope composition of crystals in Merapi basaltic-andesite and calculated melt values.

Sample I.D.	$\delta^{18}\text{O}$ (px)	$\delta^{18}\text{O}_{\text{px}}$ (melt) <sup>†</sup>	$\delta^{18}\text{O}$ (fsp)	$\delta^{18}\text{O}_{\text{fsp}}$ (melt) <sup>†</sup>	Minerals in equilibrium
M-BA98-KA1	+6.5	+6.8	n.d.	n.d.	n.d.
M-BA98-KA2	+6.8	+7.1	+7.8	+7.6	X
M-BA06-KA1	+6.9	+7.3	+7.4	+7.2	✓
M-BA06-KA2	+6.6	+6.9	+7.2	+7.0	✓
M-BA06-KA3	+5.9	+6.2	n.d.	n.d.	n.d.
M-BA06-KA4	+7.2	+7.5	+7.0	+6.8	X
M-BA06-KA5	+6.7	+7.0	+7.9	+7.7	X
M2010K plg-1	n.d.	n.d.	+6.5	+6.3	n.d.
M2010GR plg-2	n.d.	n.d.	+6.5	+6.3	n.d.
MC – cumulate	+5.4	+5.7	+6.0	+5.8	✓
MC – replicate	+5.8	+6.1	+6.2	+6.0	✓
M11-01	+5.1	+5.4	+6.3	+6.1	X
M07-53	+5.4	+5.7	+5.9	+5.7	✓

All values reported in ‰ relative to SMOW. Abbreviations: “px”, pyroxene; “fsp”, feldspar; “n.d.”, not determined. ✓: minerals in equilibrium; X: minerals in disequilibrium. Minerals in equilibrium have melt  $\delta^{18}\text{O}$  values calculated from plagioclase and pyroxene within 0.2‰.

<sup>†</sup> The  $\delta^{18}\text{O}$  (melt) is calculated assuming mineral–melt fractionation factors of  $-0.3$  and  $+0.2$  for pyroxene and feldspar, respectively (Harris et al., 2005 and references therein).

10 km. Later pyroxenes, that grew together with plagioclase, likely formed at rather shallow levels (at depths of less than 5 km).

## 6. Discussion

### 6.1. Origin of the inclusion types

The various inclusions and xenoliths (Figs. 2 and 3) provide constraints on magmatic and magma–crust interaction processes operating in the plumbing system beneath Merapi.

#### 6.1.1. Igneous and plutonic inclusions

Type (i) inclusions, i.e., ‘andesite in andesite’, reveal mixing of basaltic-andesite magmas by either self-mixing from compositionally zoned reservoirs or, more plausibly, by mixing of andesitic magmas that have evolved in different shallow storage pockets (cf. Ratdomopurbo and Poupinet, 2000; Couch et al., 2001; Gertisser and Keller, 2003b). Seismic and other geophysical investigations have not identified a large shallow magma chamber and hence a model with many but small pockets and chambers seems most reasonable (cf. Curray et al., 1977; Widiyantoro and van der Hilst, 1997; Westerhaus et al., 1998; Gertisser and Keller, 2003b; Wagner et al., 2007; Chadwick, 2008).

Type (ii) inclusions, i.e., basaltic enclaves, in turn, support mafic recharge processes (cf. Coombs et al., 2002; Troll et al., 2004). Mafic recharge is also observed as complex zoning in feldspar crystals in erupted andesites which show large variations in internal zones and frequent disequilibrium textures with their host melt, suggesting magma mixing as an integral process in Merapi’s sub-volcanic plumbing system (Gertisser and Keller, 2003b; Chadwick et al., 2007). A key realisation from this, however, is that fresh mafic magma is present beneath Merapi, although it may not erupt very frequently due to an andesite-dominated plumbing system at high levels in the crust beneath the volcano.

Types (iii), (iv), and (v) inclusions, i.e., plutonic inclusion types and amphibole megacrysts, point towards the major role of crystal fractionation and a spectrum of storage levels (or holding chambers) beneath the volcano. The big amphibole megacrysts are likely from the lower crust (cf. Davidson et al., 2007; Peters et al., 2011) and gabbros and diorites are likely lower to mid-crustal solidification products too (Chadwick, 2008). This is in line with their magmatic oxygen isotope signature (see below) and highlights the important role of recycling of older magmatic products in the Merapi system.

### 6.1.2. Metasedimentary (calc-silicate) inclusions

The non-igneous types of inclusions found in Merapi deposits comprise variably metamorphosed xenoliths of sedimentary origin. These meta-sedimentary inclusions are “true crustal xenoliths” and are foreign to the Merapi magmatic system. Their abundance in the erupted products suggests ongoing interaction between shallow magma chamber(s) and pockets and the limestone of the local upper crust. Type (vi) inclusions (calc-silicates) show frequent intense reaction and partial disintegration textures as well as vesicular andesitic domains in contact areas (Fig. 3), consistent with the concept of magma–crust interaction as a relevant process beneath Merapi.

These inclusions originate from the incorporation and thermo-metamorphic reaction of magma with limestone (e.g., Fulignati et al., 2004; Gaeta et al., 2009; Deegan et al., 2010) and leave a compositional imprint on the host magmas (Chadwick et al., 2007; Borisova et al., 2013). Reaction of limestone to diopside + wollastonite assemblages releases  $\text{CO}_2$  [ $\text{CaCO}_3$  (limestone) +  $\text{SiO}_2$  (silica)  $\rightleftharpoons$   $\text{CaSiO}_3$  (wollastonite) +  $\text{CO}_2$   $\uparrow$ ]. The liberated  $\text{CO}_2$  is, at least in theory, added to the magmatic volatile budget and likely has an impact on the volcano’s eruptive behaviour (e.g., Deegan et al., 2010; Troll et al., 2012). Judging from the frequent occurrence of calc-silicate inclusions in the Merapi lavas, and the reaction textures described above, the volatile budget of Merapi magmas may be temporarily modified prior to or during an eruption. For instance, if new reaction surfaces are created by thermal cracking, shearing, dyking, or shaking (e.g., by earthquakes, magma movement, or replenishment) this could create rapid and seemingly erratic changes in eruptive behaviour (Deegan et al., 2011).

### 6.2. Oxygen isotopes as an indicator of crustal contamination

In addition to the petrographical and petrological observations presented, oxygen isotope data are consistent with a model of crustal contamination at Merapi. The  $\delta^{18}\text{O}$  values of Merapi bulk basaltic-andesite, pyroxene, and feldspar crystals are generally elevated relative to the average Indian Ocean-type MORB value of 5.75‰ (Ito et al., 1987) and lie above bulk mixing (source contamination) arrays between Indian Ocean-type MORB-source mantle and crustal values in  $\delta^{18}\text{O}$ – $^{87}\text{Sr}/^{86}\text{Sr}$  space (Gertisser and Keller, 2003a). An exception is the bulk sample M2010-3, which has a  $\delta^{18}\text{O}$  value of  $+5.6$ ‰. The low  $\delta^{18}\text{O}$  value is correlated with high bulk Cl content, suggesting a primitive magmatic addition to this sample (see Borisova et al., 2013). Pyroxene  $\delta^{18}\text{O}$  values are higher, on average, than expected for pyroxene crystallising from a mantle-derived magma. Feldspar phenocrysts have the highest  $\delta^{18}\text{O}$  values of all the magmatic samples analysed, ranging up to 7.9‰. The high feldspar values cannot be explained by closed system Rayleigh-style fractionation (see calculated curves in Fig. 6) as this would allow for an increase in  $\delta^{18}\text{O}$  of the melt of less than 1‰ (e.g., Sheppard and Harris, 1985; Bindeman, 2008). Moreover, the frequent O-isotope disequilibrium between pyroxene and plagioclase points to different crystallisation environments for these phases.

In this respect, the material with the highest  $\delta^{18}\text{O}$  values (feldspar crystals) can provide insights into the timing of contamination within the Merapi system. Mineral barometry results (Chadwick, 2008) show that the bulk of the pyroxene in the mafic inclusions, the basaltic enclaves and the basaltic-andesite lavas at Merapi crystallised at pressures between ca. 400 and 700 MPa, which corresponds to a depth of ca. 10–25 km (Chadwick, 2008). The main interval of clinopyroxene crystallisation at Merapi is hence largely below the sedimentary part of the crust (<8 to 10 km; see van Bemmelen, 1949; Smyth et al., 2005 and references therein). Clinopyroxene in feldspar-rich felsic inclusions, however, crystallised at pressures as low as 65 MPa (Chadwick, 2008), corresponding to only the top few km of the crust. This indicates that crystallisation of a second population of pyroxene, most of the feldspar, and generation of feldspar-rich felsic inclusions is a shallow-level process and that crustal contamination occurred at the same time as feldspar crystallisation, and during magma residence

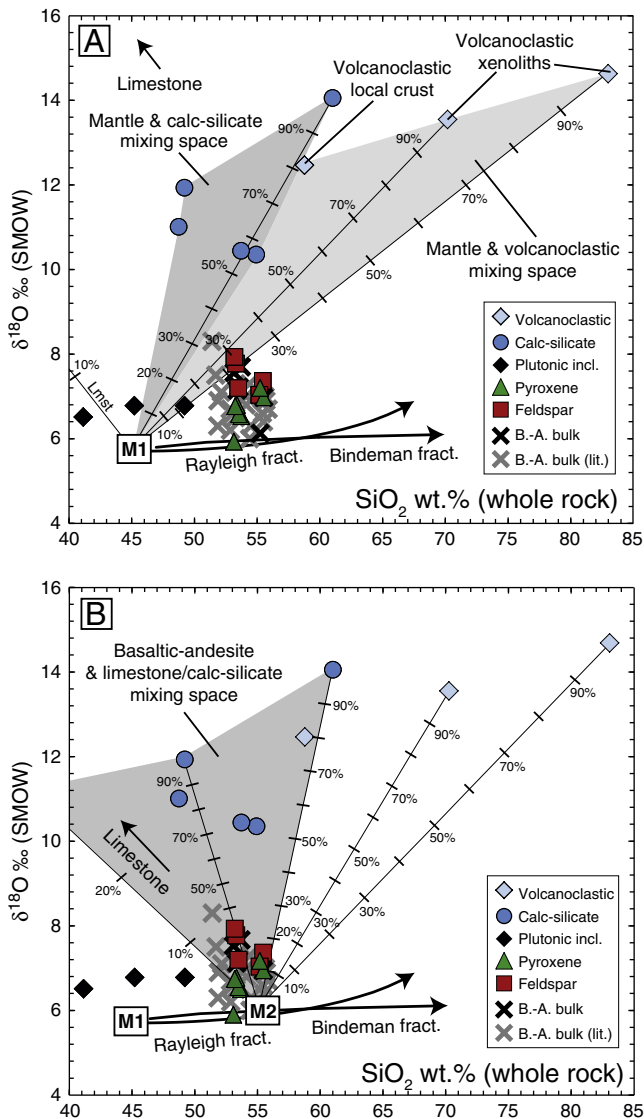


**Fig. 6.** Binary mixing models with respect to  $\delta^{18}\text{O}$  and  $\text{SiO}_2$  wt.% for Merapi samples. Mixing between an isotopically primitive mantle derived melt (M1), and various calc-silicate, limestone, and volcanoclastic compositions can reproduce the variation in the Merapi plutonic inclusion samples. However, the  $\delta^{18}\text{O}$  variation in the basaltic-andesites and the crystals within these is best explained by interaction between an already differentiated parental magma (M2, i.e., basaltic-andesite composition), and dominantly calc-silicates plus pristine limestone. The classical Rayleigh fractionation trend and the Bindeman fractionation curve (obtained by numerical crystallisation experiments; Bindeman et al., 2008) are shown to illustrate the variation in  $\delta^{18}\text{O}$  values expected from closed-system fractional crystallisation. Additional data sources: Gertisser et al. (2003a), Chadwick et al. (2007) and Troll et al. (2012).

within the top few km of the sedimentary portion of the upper crust. Earlier crystallised pyroxenes have likely seen less of this high-level contaminant (see Fig. 4).

The trends in the oxygen isotope data can then be explained by a model that involves magma–carbonate interaction during magma differentiation where crustal interaction increasingly affects the later stages of magmatic solidification in the shallow part of the system (Fig. 6). Interaction between a primitive mantle-derived parental melt and the local crust cannot reproduce the trends in the data (Fig. 6A). However, if we consider that this primitive parent differentiated to a typical Merapi basaltic-andesite composition first, and then interacted with the local carbonate crust (limestone plus calc-silicate), binary mixing models can be used to explain the measured variations (Fig. 6B). In this case, crustal interaction appears to play a limited role for the slightly elevated  $\delta^{18}\text{O}$  values of the deep pyroxene crystals, with less than 2.5% magma limestone mixing

required (Fig. 6B). The presumably shallower pyroxene crystals, in turn, record up to 20% magma calc-silicate mixing. The oxygen isotope data for both, the whole rock samples and the feldspars fall into the mixing space between differentiated basaltic andesite magma and limestone plus calc-silicates, with up to 30% crustal input recorded (Fig. 6B). Notably, calc-silicate assimilation/recycling appears as relevant as limestone interaction and the two processes likely form a continuum in the sub-volcanic environment (e.g., Gaeta et al., 2009; Deegan et al., 2010). The slightly elevated oxygen isotope values observed in plutonic inclusions, in turn, may indicate interaction between a primitive parental magma with minor amounts of either calc-silicate and/or limestone, or more likely, with older and possibly hydrated silicate crust from deeper levels (Fig. 6A).

### 6.3. Carbon isotopes in Merapi fumarole gas

Recent fumarole gases have  $\delta^{13}\text{C}_{\text{CO}_2}$  values of  $-4.4$  to  $-2.4$ ‰ (Troll et al., 2012), consistent with previously published analysis of Merapi fumarole gas of around  $-4.3$  to  $-3.9$ ‰ (e.g., Allard, 1983; Giggenbach, 1997; Toutain et al., 2009). These values (Fig. 7) show a range that includes values less negative than pure magmatic (mantle-derived)  $\text{CO}_2$  ( $\delta^{13}\text{C} \sim -5$  to  $-8$ ‰; Javoy et al., 1986; Marty and Tolstikhin, 1998; Hilton et al., 2002). The highest  $\delta^{13}\text{C}$  gas values at Merapi cannot be produced by either open or closed system magmatic degassing (cf. Holloway and Blank, 1994) meaning that an addition of a high  $\delta^{13}\text{C}$  component is required. Allard (1983) was one of the first to point out that the somewhat elevated  $\delta^{13}\text{C}$  values of Merapi fumarole gases may be caused by late-stage crustal decarbonation reactions associated with limestone assimilation. Low  $\delta^{13}\text{C}$  values of the residual carbonate in Merapi calc-silicates ( $\delta^{13}\text{C}_{\text{CO}_2} \leq -24$ ‰; see Troll et al., 2012) are the result of the loss of most of the  $\text{CO}_2$  during decarbonation (e.g., Valley, 1986). This suggests that a portion of the  $\text{CO}_2$  released by Merapi's fumaroles is derived from a non-magmatic, high- $\delta^{13}\text{C}$  source. Combining the elevated  $\delta^{13}\text{C}_{\text{CO}_2}$  values with available He isotopes, the relative contribution of the volatile sources may be estimated (Sano and Marty, 1995; Hilton et al., 2002). The Earth's mantle stores primordial He, and the average MORB-type mantle shows  $^3\text{He}/^4\text{He}$   $R_A$  of ca.  $8 \pm 1$ , while the continental crust has  $^3\text{He}/^4\text{He}$   $R_A$  of 0.1 to 0.001. Subduction of ocean crust and small portions of sediment does not significantly affect mantle He signatures in island arc lavas, such as most of the Pacific ring of fire, and yield generally mantle values. The regional values in Java indeed range from  $^3\text{He}/^4\text{He}$   $R_A = 8$  to 9 (Hilton and Craig, 1989; Sano and Marty, 1995; Goff et al., 1998; Fischer and Marty, 2005), but Merapi gas shows comparatively low  $^3\text{He}/^4\text{He}$  values of 5.5 to 6.5 ( $n = 11$ ) (Hilton and Craig, 1989; Varekamp et al., 1992; Giggenbach, 1997; Sano et al., 2001; Hilton et al., 2002; Fig. 7C). This implies variable, but at times significant, radiogenic helium additions (potentially in excess of 25 to 30%) to the Merapi gas phase via a crustal gas input (Fig. 7C).

Combining gas isotopic evidence with the petrological observations on the abundant calc-silicate xenoliths that display severe interaction textures and are strongly out-gassed ( $\delta^{13}\text{C}$  of residual carbonate in calc-silicate  $\leq -24$ ‰), the most likely source of the 'excess'  $\text{CO}_2$  is identified in form of crustal limestone during upper crustal magma storage (2–10 km). Sudden release of crustal  $\text{CO}_2$  would rapidly lead to over-pressurisation of this shallow magma reservoir and conduit system and may provide very limited and only shallow precursor seismic warning signals to volcano monitoring teams (maybe hours to days). In contrast, magmatic replenishments from depth usually travel slower and are associated with deep VT earthquakes in the weeks and months of the run up time to an eruption (e.g., Witham, 2005).

## 7. Hazard implications

Although processes such as dome crystallisation and associated internal pressure build-up have been applied to arc volcanoes to explain sudden explosive events (e.g., Stremme et al., 2011; Surono et al.,

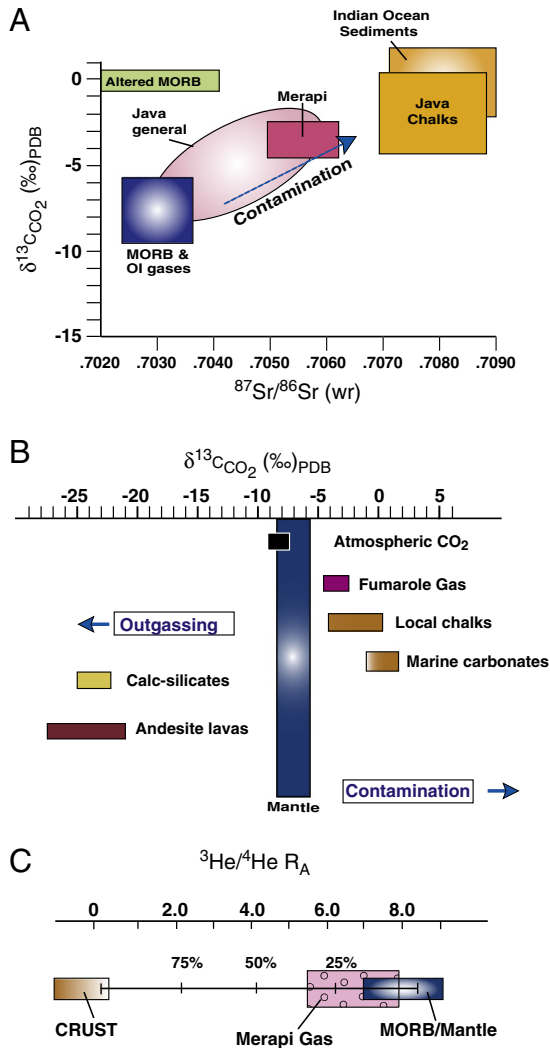


**Fig. 7.** (A)  $^{87}\text{Sr}/^{86}\text{Sr}$  whole rock vs.  $\delta^{13}\text{C}_{\text{CO}_2}$  isotope ratios for Java gas samples (modified after Allard, 1983 with updates from Gertisser and Keller, 2003a; Chadwick et al., 2007; Troll et al., 2012). Data for Java chalks is taken from Troll et al. (2012) and this study. The Merapi data field indicates contamination of volcanic gases with limestone derived  $\text{CO}_2$ , but leaves open as to whether this  $\text{CO}_2$  addition is a source contamination or a crustal contamination process. (B)  $\delta^{13}\text{C}_{\text{CO}_2}$  of rock and gas samples from Merapi compiled from literature (Hoefs, 1996; Holloway and Blank, 1994; Chadwick et al., 2007; Donoghue et al., 2008; Troll et al., 2012) and this study. Andesites and calc-silicates are strongly out-gassed, whereas the fumarole gas samples are elevated relative to lava and average mantle values, suggesting a substantial addition of limestone-derived  $\text{CO}_2$  due to magma–crust interaction. (C) He isotope ratios for Merapi gas samples ( $n=12$ ) from Allard (1983), Hilton and Craig (1989), Varekamp et al. (1992), Giggenbach (1997) and Sano et al. (2001). Mantle derived gas range and crustal He compositions are after Sano and Marty (1995) and Hilton et al. (2002). The range of Merapi data can be explained by He input from a crustal source on the order of 25 to 30%. See text for details.

2012), abundant calc-silicate xenoliths that display severe interaction textures, coupled with elevated  $\delta^{18}\text{O}$  values in phenocrysts from lavas, highly negative  $\delta^{13}\text{C}$  values in calc-silicate xenoliths, and gas  $\delta^{13}\text{C}$  values  $> -5\%$  are all consistent with carbonate assimilation as a relevant process at Merapi (Chadwick et al., 2007; Deegan et al., 2010; Troll et al., 2012; Borisova et al., 2013). Limestone degassing, in fact, is rapid and effective during carbonate assimilation, as has been successfully simulated under controlled laboratory conditions (Freda et al., 2008; Iacono-Marziano et al., 2008, 2009; Deegan et al., 2010; Mollo et al., 2010; Freda et al., 2011). Addition of limestone-derived volatiles to a shallow magma reservoir would promote vesicle formation and growth in the liquid on a short time-scale (minutes to hours), since re-dissolving  $\text{CO}_2$  back into the melt is extremely unlikely at such

shallow crustal levels (Holloway and Blank, 1994; Deegan et al., 2010). This would directly add  $\text{CO}_2$  to the free volatile phase of the system and would mainly be manifested by seismic tremors from vesiculation processes (cf. Ratdomopurbo and Poupinet, 2000). On occasion, this may increase magma chamber and conduit pressure dramatically and lead to more explosive events (cf. Proussevitch and Sahagian, 1998; Mollo et al., 2010; Deegan et al., 2011). It is conceivable that many of such  $\delta^{13}\text{C}$  additions currently go unnoticed, as they would be most pronounced during ongoing eruptive events, i.e., when fumarole sample data are, for mere safety reasons, effectively lacking (Troll et al., 2012), as is the case for the 2010 events.

The potential of limestone–magma interaction can, however, be evaluated assuming a shallow Merapi magma pocket of, e.g., 0.8 km height and up to 1.2 km width (seismic gap; Ratdomopurbo and Poupinet, 2000) or a system of ephemeral chambers of similar volume (but with higher magma–limestone contact area) that is fully enclosed in limestone units within the top 10 km of the central Javanese crust (cf. van Bemmelen, 1949; Smyth et al., 2005). Assimilation of a limestone cube with 80 m side length (10% of chamber height, see above) would produce ca.  $5.6 \times 10^5$  tonnes of  $\text{CO}_2$  (cf. Goff et al., 2001; Deegan et al., 2010), which compares to about 700 t/day on a quiet day. To deliver a similar amount of  $\text{CO}_2$  from magmatic sources, a volume of basalt magma of  $\sim 450$  m side-length would be required, which can hardly go unnoticed seismically when migrating through a volcano. Limestone assimilation in the upper crust does not require magma migration at depth, and will produce shallow seismic signals only. This is not unreasonable given the possibility of a multi-pocket plumbing system feeding Merapi volcano that also includes shallow magma storage (cf. Ratdomopurbo and Poupinet, 2000; Chadwick et al., 2007; Chadwick, 2008). Moreover, the temporally consistent petrological features of erupted lavas from Merapi was previously used to support a steady state magma system that supplies the volcano (Gertisser and Keller, 2003b), consistent with the range of plutonic textures observed (this paper). Recent seismic tomography at Merapi (Koulakov et al., 2007; Wagner et al., 2007), in fact, identified a considerable crustal anomaly beneath Merapi, but did not resolve a single, larger magma chamber. Although this anomaly suggests some 30% magma to be present and continues up to the shallowest levels beneath the volcano, individual bodies smaller than approximately  $5 \times 5$  km cannot be resolved with this approach (see e.g., Wagner et al., 2007). This implies that the most likely chamber arrangement beneath Merapi is made up of a number of magma pockets, each smaller than ca. 5 km across, that total about 30% of the crustal volume beneath the volcano. This is consistent with the common mixing features observed in Merapi's basaltic-andesites (Fig. 2; Surono et al., 2012; this study), which can be elegantly reconciled with more than one magma pocket contributing to any one of these recent eruptions.

The temporal output resulting from magma–crust interaction is, naturally, dependent on the surface area of the xenolith and the disintegration behaviour of the specific crustal wall-rock. A multi-pocket plumbing system, in this context, would offer a large surface area for interaction with wall rock and thus high levels of chemical and mechanical disintegration would allow for more rapid digestion than in the case of, e.g., a large single block digestion. Moreover, limestone assimilation can also be enhanced by regular magmatic processes such as wall rock instability caused by, e.g., thermal cracking on magma recharge, shear fracturing through magma migration, gas fracturing from local overpressure and/or through volcanic or regional seismic shocks and tremors (e.g., Chadwick et al., 2007; Harris and Ripepe, 2007; Walter et al., 2007, 2008; Deegan et al., 2010, 2011; Troll et al., 2012; Surono et al., 2012) and could thus trigger eruptions by sudden  $\text{CO}_2$  overpressurisation from disintegrating wall-rocks. This would give very limited precursor warning time, and may occur on the scale of hours to days prior to imminent changes in eruption style and intensity (Deegan et al., 2010, 2011). A late-stage crustal volatile addition to purely mantle and slab-derived volatile sources by shallow-level contamination could thus sustain and intensify eruptions independently of magmatic recharge or

fractional crystallisation by sudden over-pressurisation and consequent increased gas release from shallow chambers and eruptive conduits (e.g., Troll et al., 2012). This contrasts with much slower magmatic replenishments from depth that will be associated with deep VT earthquakes in the weeks to months of run up time to an eruption (e.g., Hidayat et al., 2000; Ratdomopurbo and Poupinet, 2000).

## Acknowledgements

Field-work as early as 2002 (for 1994 and 1998 deposits) was planned and carried out with the support of scientists of the Direktorat Vulkanologi, Merapi (BPPTK), particularly A. Ratdomopurbo and by scientists from the Volcanological Survey of Indonesia, especially A. Purbawianta, and a number of individuals from Yogyakarta, particularly M. Mahjum and M. Taufiq. Discussions with L. Dallai, J. Davidson, B. Lühr, C. MacPherson, T.R. Walter, and B. Zimanowski, are highly appreciated. C. Buckley, L. McCourt, and F. Rawoat are thanked for assistance during data processing and evaluation. Constructive journal reviews by C. Siebe, P. Jousset, and an anonymous referee are gratefully acknowledged. We also thank the Mineralogical Society of Great Britain and Ireland (Min Soc), Enterprise Ireland (EI), the Swedish Science Foundation (VR), the European Commission (EC), the Deutsche Forschungsgemeinschaft (DFG), the UK Natural Environmental Research Council (NERC), the National Research Foundation of South Africa, and the Centre for Natural Disaster Sciences (CNDS) at Uppsala University for their generous financial support.

## References

- Allard, P., 1983. The origin of hydrogen, carbon, sulphur, nitrogen and rare gases in volcanic exhalations: evidence from isotope geochemistry. In: Tazieff, H., Sabroux, J. (Eds.), *Forecasting Volcanic Events*. Elsevier, New York, pp. 337–386.
- Andreastuti, S.D., Alloway, B.V., Smith, I.M., 2000. A detailed tephrostratigraphic framework at Merapi Volcano, Central Java, Indonesia: implications for eruption predictions and hazard assessment. *Journal of Volcanology and Geothermal Research* 100, 51–67.
- Arculus, R.J., Johnson, R.W., 1981. Island arc magma sources: a geochemical assessment of the roles of slab derived components and crustal contamination. *Geochemical Journal* 15, 109–133.
- Arculus, R.J., Powell, R., 1986. Source component mixing in the regions of arc magma generation. *Journal of Geophysical Research* 91, 5913–5926.
- Bindeman, I., 2008. Oxygen isotopes in mantle and crustal magmas as revealed by single crystal analysis. *Reviews in Mineralogy and Geochemistry* 69, 445–478.
- Bindeman, I., Gurenko, A., Sigmarsson, O., Chaussidon, M., 2008. Oxygen isotope heterogeneity and disequilibria of olivine crystals in large volume Holocene basalts from Iceland: evidence for magmatic digestion and erosion of Pleistocene hyaloclastites. *Geochimica et Cosmochimica Acta* 72, 4397–4420.
- Borisova, A.Y., Martel, C., Gouy, S., Pratomo, I., Sumarti, S., Toutain, J.-P., Bindeman, I.N., de Parseval, P., Metaxian, J.-P., Surono, S., 2013. Highly explosive 2010 Merapi eruption: Evidence for shallow-level crustal assimilation and hybrid fluid. *Journal of Volcanology and Geothermal Research* 261, 193–208.
- Borthwick, J., Harmon, R.S., 1982. A note regarding  $\text{C1F}_3$  as an alternative to BrF<sub>3</sub> for oxygen isotope analysis. *Geochimica et Cosmochimica Acta* 46, 1665–1668.
- Bowen, N.L., 1928. *The Evolution of the Igneous Rocks*. Princeton University Press, Princeton, pp. 1–132.
- Budi-Santoso, A., Lesage, P., Dwiyo, S., Sumarti, S., Subandriyo, Surono, Jousset, P., Metaxian, J.-P., 2013. Analysis of the seismic activity associated with the 2010 eruption of Merapi Volcano, Java. *Journal of Volcanology and Geothermal Research* 261, 153–170.
- Camus, G., Gourgaud, A., Mossand-Berthommier, P.-C., Vincent, P.-M., 2000. Merapi (Central Java, Indonesia): an outline of the structural and magmatological evolution, with a special emphasis to the major pyroclastic events. *Journal of Volcanology and Geothermal Research* 100, 139–163.
- Chadwick, J.P., 2008. Magma crust interaction in volcanic systems: Case studies from Merapi Volcano, Indonesia, Taupo Volcanic Zone, New Zealand, and Slieve Gullion, N. Ireland. PhD thesis, Trinity College Dublin, pp. 52–181.
- Chadwick, J.P., Troll, V.R., Ginibre, C., Morgan, D., Gertisser, R., Waight, T.E., Davidson, J.P., 2007. Carbonate assimilation at Merapi Volcano, Java, Indonesia: insights from crystal isotope stratigraphy. *Journal of Petrology* 48, 1793–1812.
- Charbonnier, S.J., Gertisser, R., 2008. Field observations and surface characteristics of pristine block-and-ash flow deposits from the 2006 eruption of Merapi Volcano, Java, Indonesia. *Journal of Volcanology and Geothermal Research* 177, 971–982.
- Chiba, H., Chacko, T., Clayton, R.N., Goldsmith, J.R., 1989. Oxygen isotope fractionations involving diopside, forsterite, magnetite, and calcite: applications to geothermometry. *Geochimica et Cosmochimica Acta* 53, 2985–2995.
- Clocchiatti, R., Joron, J.-L., Kerinac, F., 1982. Quelques données préliminaires sur la lave du dôme actuel du volcan Merapi (Java, Indonésie) et sur ses enclaves. *Comptes-Rendus des Seances de l'Académie des Sciences* 295, 817–822.
- Combs, M.L., Eichelberger, J.C., Rutherford, M.J., 2002. Experimental and textural constraints on mafic enclave formation in volcanic rocks. *Journal of Volcanology and Geothermal Research* 119, 125–144.
- Couch, S., Sparks, R.S.J., Caroll, M.R., 2001. Mineral disequilibrium in lavas explained by convective self-mixing in open magma chambers. *Nature* 411, 1037–1039.
- Curry, J.R., Shor, G.G., Raitt, R.W., Henry, M., 1977. Seismic refraction and reflection studies of crustal structure of the eastern Sunda and western Banda arcs. *Journal of Geophysical Research* 82, 2479–2489.
- Davidson, J.P., 1995. Mechanisms of contamination in Lesser Antilles island arc magmas from radiogenic and oxygen isotope relationships. *Earth and Planetary Science Letters* 72, 163–174.
- Davidson, J.P., McMillan, N.J., Moorbath, S., Wörner, G., Russell, S.H., Lopez-Escobar, L., 1990. The Nevados de Payachata volcanic region (18° S/69° W, N. Chile) II. Evidence for widespread crustal involvement in Andean magmatism. *Contributions to Mineralogy and Petrology* 105, 412–432.
- Davidson, J., Turner, S., Handley, H., Macpherson, C., Dosseto, A., 2007. Amphibole 'sponge' in arc crust? *Geology* 35, 787–790.
- Debaillie, V., Doucelance, R., Weiss, D., Schiano, P., 2006. Multi-stage mixing in subduction zones: application to Merapi Volcano, (Java Island, Sunda arc). *Geochimica et Cosmochimica Acta* 70, 723–741.
- Deegan, F.M., Troll, V.R., Freda, C., Misiti, V., Chadwick, J.P., McLeod, C.L., Davidson, J.P., 2010. Magma–carbonate interaction processes and associated CO<sub>2</sub> release at Merapi Volcano, Indonesia: insights from experimental petrology. *Journal of Petrology* 51, 1027–1051.
- Deegan, F.M., Troll, V.R., Freda, C., Misiti, V., Chadwick, J.P., 2011. Fast and furious: crustal CO<sub>2</sub> release at Merapi Volcano, Indonesia. *Geology Today* 27, 63–64.
- Donoghue, E., Troll, V.R., Schwarzkopf, L.M., Clayton, G., Goodhue, R., 2008. Organic block coatings in block-and-ash flow deposits at Merapi Volcano, central Java. *Geological Magazine* 146, 113–120.
- Donovan, K., Suharyanto, A., 2011. The creatures will protect us. *Geoscientist* 21, 12–17.
- Eiler, J.M., Crawford, A., Elliott, T., Farley, K.A., Valley, J.W., Stolper, E.M., 2000. Oxygen isotope geochemistry of oceanic arc lavas. *Journal of Petrology* 41, 229–256.
- Ellam, R.M., Harmon, R.S., 1990. Oxygen isotope constraints on the crustal contribution to the subduction-related magmatism of the Aeolian islands, southern Italy. *Journal of Volcanology and Geothermal Research* 44, 105–122.
- Fagereng, Å., Harris, C., La Grange, M., Stevens, G., 2008. Stable isotope study of the Archean rocks of the Vredefort structure central Kaapvaal Craton, South Africa. *Contributions to Mineralogy and Petrology* 155, 63–78.
- Fischer, T.P., Marty, B., 2005. Volatile abundance in the sub-arc mantle: insights from volcanic and hydrothermal gas discharges. *Journal of Volcanology and Geothermal Research* 140, 205–216.
- Freda, C., Gaeta, M., Misiti, V., Mollo, S., Dolfi, D., Scarlato, P., 2008. Magma–carbonate interaction: an experimental study on ultrapotassic rocks from Alban Hills (Central Italy). *Lithos* 101, 397–415.
- Freda, C., Gaeta, M., Giaccio, B., Marra, F., Palladino, D.M., Scarlato, P., Sottili, G., 2011. CO<sub>2</sub>-driven large mafic explosive eruptions: the Pozzolane Rosse case study from the Colli Albani Volcanic District (Italy). *Bulletin of Volcanology* 73, 241–256.
- Fulginiti, P., Marianelli, P., Santacroce, R., Sbrana, A., 2004. Probing the Vesuvius magma chamber–host rock interface through xenoliths. *Geological Magazine* 141, 417–428.
- Gaeta, M., Di Rocco, T., Freda, C., 2009. Carbonate assimilation in open magmatic systems: the role of melt-bearing skarns and cumulate forming processes. *Journal of Petrology* 50, 361–385.
- Gertisser, G., Keller, J., 2003a. Trace element and Sr, Nd, Pb and O isotope variations in medium-K and high-K volcanic rocks from Merapi Volcano, Central Java, Indonesia: evidence for the involvement of subducted sediments in Sunda Arc magma genesis. *Journal of Petrology* 44, 457–489.
- Gertisser, R., Keller, J., 2003b. Temporal variations in magma composition at Merapi Volcano (Central Java, Indonesia): magmatic cycles during the past 2000 years of explosive activity. *Journal of Volcanology and Geothermal Research* 123, 1–23.
- Gertisser, R., Charbonnier, S.J., Keller, J., Quidelleur, X., 2012. The geological evolution of Merapi volcano, Central Java, Indonesia. *Bulletin of Volcanology* 74, 1213–1233. <http://dx.doi.org/10.1007/s00445-012-0591-3>.
- Giggenbach, W.F., 1997. Fifth field workshop on volcanic gases, Java, 18–29 July 1994: preliminary evaluation of analytical results II. *IAVCEI Commun. Chemistry of Volcanic Gases Newsletter* 12, 4–10.
- Goff, F., Janik, C.J., Delgado, H., Werner, C., Counce, D., Stimac, J.A., Siebe, C., Love, S.P., Williams, S.N., Fischer, T., Johnson, L., 1998. Geochemical surveillance of magmatic volatiles at Popocatepetl Volcano, Mexico. *GSA Bulletin* 6, 695–710.
- Goff, F., Love, S.P., Warren, R.G., Counce, D., Obenholzer, J., Siebe, C., Schmidt, S.C., 2001. Passive infrared remote sensing evidence for large, intermittent CO<sub>2</sub> emissions at Popocatepetl Volcano, Mexico. *Chemical Geology* 177, 133–156.
- Gregory, R.T., Criss, R.E., 1986. Isotopic exchange in open and closed systems. In: Valley, J.W., Taylor Jr., H.P., O'Neil, J.R. (Eds.), *Stable Isotopes in High Temperature Geological Processes*. Reviews in Mineralogy 16, 91–127.
- Gregory, R.T., Criss, R.E., Taylor Jr., H.P., 1989. Oxygen isotope exchange kinetics of mineral pairs in closed and open systems: applications to problems of hydrothermal alteration of igneous rocks and Precambrian iron formations. *Chemical Geology* 75, 1–42.
- Hamilton, W., 1979. Tectonics of the Indonesian region. *U.S. Geological Survey Professional Paper* 1078, 1–345.
- Harris, A.J.L., Ripepe, M., 2007. Regional earthquake as a trigger for enhanced volcanic activity: evidence from MODIS thermal data. *Geophysical Research Letters* 34, 1–6.
- Harris, C., Vogeli, J., 2010. Oxygen isotope composition of garnet in the Peninsula Granite, Cape Granite Suite, South Africa: constraints on melting and emplacement mechanisms. *South African Journal of Geology* 113, 401–412.
- Harris, C., Smith, H.S., le Roex, A.P., 2000. Oxygen isotope composition of phenocrysts from Tristan da Cunha and Gough Island lavas: variation with fractional crystallization and evidence for assimilation. *Contributions to Mineralogy and Petrology* 138, 164–175.

- Harris, C., Pronost, J.J.M., Ashwal, L.D., Cawthorn, R.G., 2005. Oxygen and hydrogen isotope stratigraphy of the Rustenburg layered suite, Bushveld Complex: constraints on crustal contamination. *Journal of Petrology* 46, 579–601.
- Hidayat, D., Voight, B., Langston, C., Ratdomopurbo, A., Ebeling, C., 2000. Broadband seismic experiment at Merapi Volcano, Java, Indonesia: very-long-period pulses embedded in multiphase earthquakes. *Journal of Volcanology and Geothermal Research* 100, 215–231.
- Hildreth, W., Moorbath, S., 1988. Crustal contributions to arc magmatism in the Andes of Chile. *Contributions to Mineralogy and Petrology* 98, 455–489.
- Hilton, D.R., Craig, H., 1989. A helium isotope transect along the Indonesian archipelago. *Nature* 342, 906–908.
- Hilton, D.R., Fischer, T.P., Marty, B., 2002. Noble gases in subduction zones and volatile recycling. *Reviews in Mineralogy and Geochemistry* 47, 319–370.
- Hoefs, J., 1996. *Stable Isotopes*. Springer Verlag, Berlin, p. 201.
- Holloway, J.R., Blank, J.G., 1994. Application of experimental results to C–O–H species in natural melts. *Reviews in Mineralogy* 30, 187–230.
- Iacono-Marziano, G., Gaillard, F., Pichavant, M., 2008. Limestone assimilation by basaltic magmas: an experimental re-assessment and application to Italian volcanoes. *Contributions to Mineralogy and Petrology* 155, 719–738.
- Iacono-Marziano, G., Gaillard, F., Scaillet, B., Pichavant, M., Chiodini, G., 2009. Role of non-mantle CO<sub>2</sub> in the dynamics of volcano degassing: the Mount Vesuvius example. *Geology* 37, 319–322.
- Ito, E., White, W.M., Göpel, C., 1987. The O, Sr, Nd and Pb isotope geochemistry of MORB. *Chemical Geology* 62, 157–176.
- Itoh, H., Takahama, J., Takahashi, M., Miyamoto, K., 2000. Hazard estimation of the possible pyroclastic flow disasters using numerical simulation related to the 1994 activity at Merapi Volcano. *Journal of Volcanology and Geothermal Research* 100, 503–516.
- Jarrard, R.D., 1986. Relations among subduction parameters. *Reviews of Geophysics* 24, 217–284.
- Javoy, M., Pineau, F., Delorme, H., 1986. Carbon and nitrogen isotopes in the mantle. *Chemical Geology* 57, 41–62.
- Jousset, P., Budi-Santoso, A., Jolly, A.D., Boichu, M., Surono, Dwiyo, S., Sumarti, S., Hidayati, S., Thierry, P., 2013. Signs of magma ascent in LP and VLP seismic events and link to degassing: An example from the 2010 explosive eruption at Merapi volcano, Indonesia. *Journal of Volcanology and Geothermal Research* 261, 171–192.
- Koulakov, I., Bohm, M., Asch, G., Lüher, B.-G., Manzanera, A., Brotopuspito, K.S., Fauzi, P., Purbawinata, M.A., Puspito, N.T., Ratdomopurbo, A., Kopp, H., Rabbel, W., Sheykhunova, E., 2007. P and S velocity structure of the crust and the upper mantle beneath central Java from local tomography inversion. *Journal of Geophysical Research* 112, B08310. <http://dx.doi.org/10.1029/2006JB004712>.
- Kyser, T.K., O'Neil, J.R., Carmichael, I.S.E., 1981. Oxygen isotope thermometry of basic lavas and mantle nodules. *Contributions to Mineralogy and Petrology* 77, 11–23.
- Marty, B., Tolstikhin, I.N., 1998. CO<sub>2</sub> fluxes from mid-ocean ridges, arcs and plumes. *Chemical Geology* 145, 233–248.
- Mollo, S., Gaeta, M., Freda, C., Di Rocco, T., 2010. Carbonate assimilation in magmas: a reappraisal based on experimental petrology. *Lithos* 114, 503–514.
- Newhall, C.G., Bronto, S., Alloway, B., Banks, N.G., Bahar, I., del Marmol, M.A., Hadasantono, R.D., Holcomb, R.T., McGeekin, J., Miksic, J.N., Rubin, M., Sayudi, S.D., Sukhyar, R., Andreaastuti, S., Tilling, R.L., Torley, R., Trimble, D., Wirakusumah, A.D., 2000. 10,000 Years of explosive eruptions of Merapi Volcano, Central Java: archeological and modern implications. *Journal of Volcanology and Geothermal Research* 100, 9–50.
- Peters, S.T.M., Chadwick, J.M., Troll, V.T., 2011. Amphibole antecrysts in deposits of Merapi Volcano, Indonesia: a plutonic phase in extrusive magmas. *Goldschmidt supplement. Mineralogical Magazine* 75 (3), A1627.
- Plank, T., Langmuir, C.H., 1998. The chemical composition of subducting sediment and its consequences for the crust and mantle. *Chemical Geology* 145, 325–394.
- Potts, A.J., Midgley, J.J., Harris, C., 2009. Stable isotope and <sup>14</sup>C study of biogenic calcrite in a termite mound, Western Cape, South Africa and its palaeoenvironmental significance. *Quaternary Research* 72, 258–264.
- Preece, K., Barclay, J., Gertisser, R., Herd, R.A., 2013. Textural and micro-petrological variations in the eruptive products of the 2006 dome-forming eruption of Merapi volcano, Indonesia: Implications for sub-surface processes. *Journal of Volcanology and Geothermal Research* 261, 98–120.
- Proussevitch, A., Sahagian, D., 1998. Dynamics and energetics of bubble growth in magmas: analytical formulation and numerical modelling. *Journal of Geophysical Research* 103, 18223–18251.
- Ratdomopurbo, A., Poupinet, G., 2000. An overview of the seismicity of Merapi Volcano (Java, Indonesia), 1983–1994. *Journal of Volcanology and Geothermal Research* 100, 193–214.
- Richter, G., Wassermann, J., Zimmer, M., Ohrnberger, M., 2004. Correlation of seismic activity and fumarole temperature at the Mt. Merapi Volcano (Indonesia) in 2000. *Journal of Volcanology and Geothermal Research* 135, 331–342.
- Sano, Y., Marty, B., 1995. Origin of carbon in fumarolic gas from island arcs. *Chemical Geology* 119, 265–274.
- Sano, Y., Takahata, N., Nishio, Y., Fischer, T.P., Williams, S.N., 2001. Volcanic flux of nitrogen from the Earth. *Chemical Geology* 171, 263–271.
- Schwarzkopf, L.M., Schmincke, H.-U., Cronin, S.J., 2005. A conceptual model for block-and-ash flow basal avalanche transport and deposition, based on deposit architecture of 1998 and 1994 Merapi flows. *Journal of Volcanology and Geothermal Research* 139, 117–134.
- Sheppard, S.M.F., Harris, C., 1985. Hydrogen and oxygen isotope geochemistry of Ascension Island lavas and granites: variation with crystal fractionation and interaction with seawater. *Contributions to Mineralogy and Petrology* 91, 74–81.
- Smyth, H.R., Hall, R., Hamilton, J., Kinny, P., 2005. East Java: Cenozoic basins, volcanoes and ancient basement. *Proceedings, Indonesian Petroleum Association, Thirtieth Annual Convention & Exhibition*.
- Stremel, W., Ortega, I., Siebe, C., Grutter, M., 2011. Gas composition of Popocatepetl Volcano between 2007 and 2008: FTIR spectroscopic measurements of an explosive event and during quiescent degassing. *Earth and Planetary Science Letters* 301, 502–510.
- Surono, Jousset, P., Pallister, J., Boichu, M., Fabrizia, M., Buongiorno, M.F., Budisantoso, A., Costa, F., Andreaastuti, S., Prata, F., Schneider, D., Clarisse, L., Humaida, H., Sumarti, S., Bignami, C., Griswold, J., Carn, S., Oppenheimer, C., Lavigne, F., 2012. The 2010 explosive eruption of Java's Merapi Volcano – a '100-year' event. *Journal of Volcanology and Geothermal Research* 241–242, 121–135.
- Thirlwall, M.F., Graham, A.M., Arculus, R.J., Harmon, R.S., Macpherson, C.G., 1996. Resolution of the effects of crustal assimilation, sediment subduction and fluid transport in island arc magmas; Pb–Sr–Nd–O isotope geochemistry of Grenada, Lesser Antilles. *Geochimica et Cosmochimica Acta* 60, 4785–4810.
- Thouret, J.-C., Lavigne, F., Kelfoun, K., Bronto, S., 2000. Toward a revised hazard assessment at Merapi Volcano, Central Java. *Journal of Volcanology and Geothermal Research* 100, 479–502.
- Toutain, J.-P., Sortino, F., Baubron, J.-C., Richon, P., Surono Sumarti, S., Nonell, A., 2009. Structure and CO<sub>2</sub> budget of Merapi Volcano during inter-eruptive periods. *Bulletin of Volcanology* 71, 815–826.
- Troll, V.R., Donaldson, C.H., Emeleus, C.H., 2004. Pre-eruptive magma mixing in ash-flow deposits of the Rum Igneous Centre, Scotland. *Contributions to Mineralogy and Petrology* 147, 722–739.
- Troll, V.R., Hilton, D.R., Jolis, E.M., Chadwick, J.P., Blythe, L.S., Deegan, F.M., Schwarzkopf, L.M., Zimmer, M., 2012. Crustal CO<sub>2</sub> liberation during the 2006 eruption and earthquake events at Merapi Volcano, Indonesia. *Geophysical Research Letters* 39, L11302. <http://dx.doi.org/10.1029/2012GL051307>.
- Turner, S., Foden, J., 2001. U, Th and Ra disequilibria, Sr, Nd and Pb isotopes and trace element variations in Sunda arc lavas: predominance of a subducted sediment component. *Contributions to Mineralogy and Petrology* 142, 43–57.
- Valley, J.W., 1986. Stable isotope geochemistry of metamorphic rocks. In: Valley, J.W., Taylor, H.P., Jr., O'Neil, J.R. (Eds.), *Stable isotopes in high temperature geological processes*. *Reviews in Mineralogy* 16, 445–490.
- van Bemmelen, R.W., 1949. *The Geology of Indonesia. : General Geology, vol. 1A*. Government Printing Office, The Hague.
- Varekamp, J.C., Kreulen, R., Poorter, R.P.E., Van Bergen, M.J., 1992. Carbon sources in arc volcanism, with implications for the carbon cycle. *Terra Nova* 4, 363–373.
- Vennemann, T.W., Smith, H.S., 1990. The rate and temperature of reaction of CLF<sub>3</sub> with silicate minerals, and their relevance to oxygen isotope analysis. *Chemical Geology* 86, 83–88.
- Voight, B., Constantine, E.K., Siswoidjono, S., Torley, R., 2000. Historical eruptions of Merapi Volcano, Central Java, Indonesia, 1768–1998. *Journal of Volcanology and Geothermal Research* 100, 69–138.
- Wagner, D., Koulakov, I., Rabbel, W., Luehr, B.-G., Wittwer, A., Kopp, H., the MERAMEX Scientists, 2007. Joint Inversion of active and passive seismic data in Central Java. *Geophysical Journal International* 170, 923–932.
- Walter, T.R., Wang, R., Zimmer, M., Gresser, H., Luehr, B., Ratdomopurbo, A., 2007. Volcanic activity influenced earthquakes: static dynamic stress triggering at Mt. Merapi. *Geophysical Research Letters* 34, 1–5.
- Walter, T.R., Wang, R., Luehr, B.-G., Wassermann, J., Behr, Y., Parolai, S., Anggraini, A., Günther, E., Sobiesiak, M., Gresser, H., Wetzel, H.-U., Milkereit, C., Sri Brotopuspito, P.J.K., Harjadi, P., Zschau, J., 2008. The 26 May 2006 magnitude 6.4 Yogyakarta earthquake south of Merapi Volcano: did lahar deposits amplify ground shaking and thus to the disaster? *Geochemistry, Geophysics, Geosystems* 9, 1–9.
- Westerhaus, M., Rebscher, D., Welle, W., Pfaff, A., Körner, A., Nandaka, I.G.M., 1998. Deformation measurements at the flanks of Merapi Volcano. *Deutsche Geophysikalische Gesellschaft, Mitteilungen, Sonderband III*, pp. 3–8.
- Widiyantoro, S., van der Hilst, R., 1997. Mantle structure beneath Indonesia inferred from high-resolution tomographic imaging. *Geophysical Journal International* 130, 167–182.
- Wilson, M., 1997. *Igneous Petrogenesis*. Chapman and Hall, London, pp. 1–456.
- Witham, C.S., 2005. Volcanic disasters and incidents: a new database. *Journal of Volcanology and Geothermal Research* 148, 191–233.